Available online at www.sciencedirect.com
SCIENCE DIRECT®
ELSEVIER
Journal of Crystal Growth 285 (2005) 561–565
JOURNAL OF CRYSTAL GROWTH
www.elsevier.com/locate/jcrysgro

Highly aligned ZnS nanorods grown by plasma-assisted metalorganic chemical vapor deposition

Q.J. Feng[a,b], D.Z. Shen[a,*], J.Y. Zhang[a], H.W. Liang[c], D.X. Zhao[a], Y.M. Lu[a], X.W. Fan[a]

[a]*Key Laboratory of Excited State Processes, Chinese Academy of Sciences, Changchun Institute of Optics, Fine Mechanics and Physics, Chinese Academy of Sciences, 16- Dongnanhu Road, Changchun 130033, P.R. China*
[b]*Graduate School of the Chinese Academy of Sciences, P.R. China*
[c]*Department of Physics, Dalian University of Technology, 2-Lingshui Road, Dalian 116023, P.R. China*

Received 25 March 2005; received in revised form 24 July 2005; accepted 5 September 2005
Available online 24 October 2005
Communicated by J.M. Redwing

Abstract

ZnS nanorods were grown on *c*-plane Al_2O_3 substrate by plasma-assisted metalorganic chemical vapor deposition without employing any metal catalyst. By adjusting the reactor pressure in the growth chamber, vertical-aligned ZnS nanorod arrays were obtained under lower pressure of 10 Torr. The images of field-emission scanning electron microscope and transmission electron microscopy of ZnS show that the obtained ZnS nanorods have a uniform diameter of 60 nm with the length of about 400 nm. Selected-area electron diffraction pattern and X-ray diffraction measurements indicate that ZnS nanorods are single crystals with a hexagonal structure. In photoluminescence spectrum, a strong near band-edge emission located at 335 nm was observed, which indicates that the nanorods are of high-optical quality.

PACS: 81.15.Gh; 78.67.Lt; 78.67.−n

Keywords: A1. Nanostructure; A3. Metalorganic chemical vapor deposition; B1. Zinc compounds; B2. Semiconducting II–VI materials

1. Introduction

One-dimensional (1D) nanoscale semiconductor structures, such as nanowires, nanobelts, and nanorods, have attracted considerable attention due to their interesting fundamental properties and potential applications in nanoscale

*Corresponding author. Tel.: +86 431 6176322; fax: +86 431 4627031.
E-mail address: qjf916@sohu.com (Q.J. Feng).

0022-0248/$ - see front matter © 2005 Elsevier B.V. All rights reserved.
doi:10.1016/j.jcrysgro.2005.09.003

opto-electronic devices [1]. ZnS, an important semiconductor compound, has wide band-gap energy of 3.7 eV at 300 K [2]. It has been used as emitter in photoluminescence (PL) [3], electroluminescence [4], mechanoluminescence [5], acousticluminescence [6], and thermal luminescence [7]. ZnS also has wide applications in the fields of displays, sensors, lasers [8], and photocatalysis [9]. The ZnS in nanoscale has been reported to have some characteristics different from the bulk crystal, which may extend its application range [10]. Recently, various ZnS nanostructures have been synthesized. For instance, nanowires [11–13], nanosheets [14,15], nanobelts [16,17], nanorods [18], nanoribbons [10,19], and nanotubes [20], etc. Most 1D ZnS nanostructures were grown using a thermal evaporation method with Au catalyst following vapor–liquid–solid (VLS) growth mechanism. In VLS growth process, catalysts play an essential role by forming liquid alloy droplet to provide nucleation sites for 1D nanostructure growth [21]. However, even low defect concentrations affect physical properties of semiconductors and unintentionally doped impurities are detrimental to device fabrication [22].

In this article, we reported a catalyst-free method to grow vertical aligned ZnS nanorods array. The ZnS nanorods were fabricated by plasma-assisted metalorganic chemical vapor deposition (P-MOCVD). MOCVD is of particular interest since it has many advantages such as feasibility of large area growth as well as simple and accurate doping and thickness control. At present, the vertically well-aligned ZnO nanorods [22], and nanotips [23] have been successfully prepared by using this technique. As far as we know, ZnS nanorods grown by P-MOCVD have not been reported. To determine the growth condition of ZnS nanorods, the experiment was operated under various growth pressure but the other growth parameters were fixed. Obtained ZnS nanorods were investigated further to characterize the structural and optical properties.

2. Experimental procedure

ZnS nanorods were grown on *c*-plane Al_2O_3 substrates by a self-assemble P-MOCVD system at substrate temperature of 650 °C without employing any metal catalyst. To obtain the optimum growth parameters of ZnS nanorods, growth pressures were fixed to 35, 24, 16 and 10 Torr. High-purity hydrogen was used as carrier gas to transfer the reactants into the reaction chamber with a horizontal rectangular quartz reactor and the total gas flow rate was kept at 2 L/min. Dimethylzinc (DMZn) and H_2S were used as reaction precursors. Growth time of samples in the reaction chamber was 50 min. The plasma of our MOCVD equipment was produced by high-frequency inductive loop, which enlaced outside quartz growth chamber. This high-frequency loop could heat up substrates. And plasma generation depended strongly on both growth temperature and reactor pressure.

The crystal structure of ZnS nanorods was investigated by X-ray diffraction (XRD) including $\theta - 2\theta$ scan and selected-area electron diffraction (SAED). Surface morphology of samples was examined using a field emission scanning electron microscope (FE–SEM) and transmission electron microscopy (TEM). PL spectroscopy measurement was carried out under the condition of excitation by a He–Cd laser (325 nm).

3. Results and discussion

Fig. 1 shows FE–SEM images of ZnS nanostructures fabricated under different reactor pressures at 650 °C. At a reactor pressure of 35 Torr, a ZnS thin film with rough surface was observed, as show in Fig. 1(a). This thin film consists of nanoislands with a diameter around 200 nm. Fig. 1(b) shows the meshwork structure of ZnS obtained at 24 Torr, which is composed of congregating ZnS nanograins. As the growth pressures decreases to 16 Torr, ZnS nanorods with diameters of 70–120 nm present on the substrate surface. The lengths of nanorods are in range of 100–300 nm. Finally, when reactor pressure reached to 10 Torr, highly vertical aligned ZnS nanorods were obtained, as shown in Fig. 1(d). Sizes of the nanorods were given in the images of TEM, as seen in Fig. 3. Moreover, Fig. 1(d) also

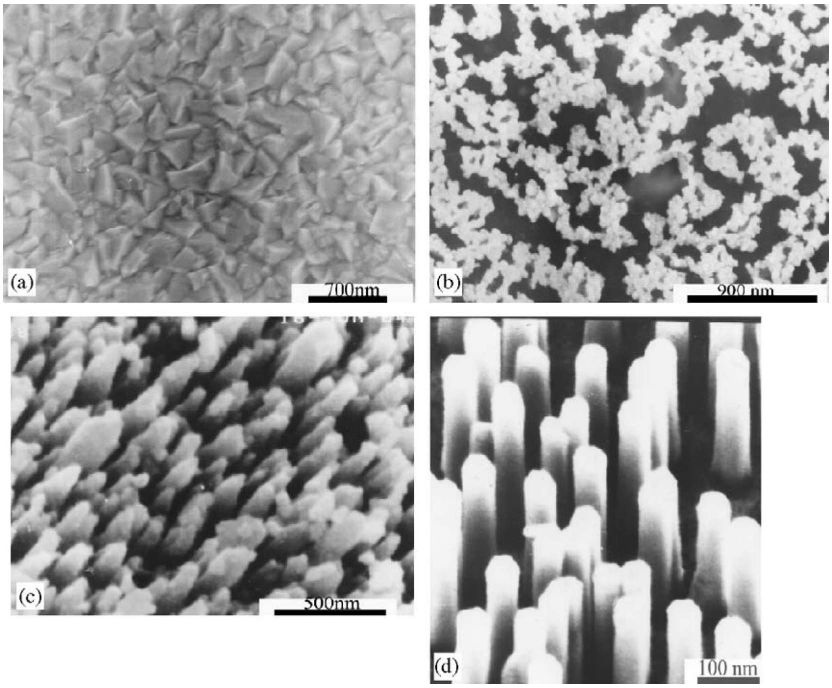

Fig. 1. FE–SEM images of ZnS nanostructure formed at 650 °C under different reactor pressures: (a) 35 Torr, (b) 24 Torr, (c) 16 Torr and (d) 10 Torr.

revealed that the distributions of nanorods in diameters, lengths, and densities are uniform.

By analyzing XRD patterns all the ZnS nanostructures are wurtzite structure at different growth pressure. Fig. 2 shows the XRD pattern of ZnS nanorods grown on *c*-plane sapphire substrates at reactor pressures of 10 Torr. In Fig. 2 only ZnS (0 0 2) and Al_2O_3 (0 0 6) diffraction peaks were detected at 28.61° and 41.67°, respectively, which indicated that the highly oriented hexagonal (wurtzite) nanorods were grown with heterogeneous in-plane alignments as well as *c*-axis orientation.

The morphology and structure of ZnS nanorods were characterized in further detail by TEM and SAED. Fig. 3 shows the TEM image of nanorods grown at reactor pressure of 10 Torr. The insert is the SAED pattern of a single ZnS nanorod. It is clearly seen that the ZnS nanorods with diameters and lengths of about 55–60 and 350–400 nm, respectively, were obtained. The bright diffraction spots in the SAED pattern indicate that the ZnS nanorods are single crystalline structure [24].

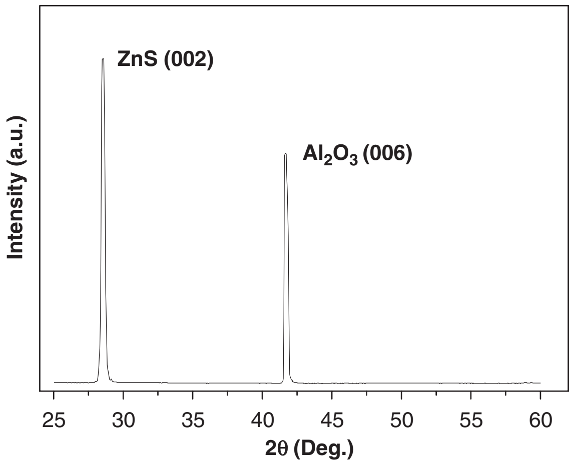

Fig. 2. The XRD pattern of ZnS nanorods grown on *c*-sapphire substrates at reactor pressures of 10 Torr.

The different morphologies of all products are believably related to the influence of plasma energy on the reaction precursors. Because in the experiment no special plasma generator is

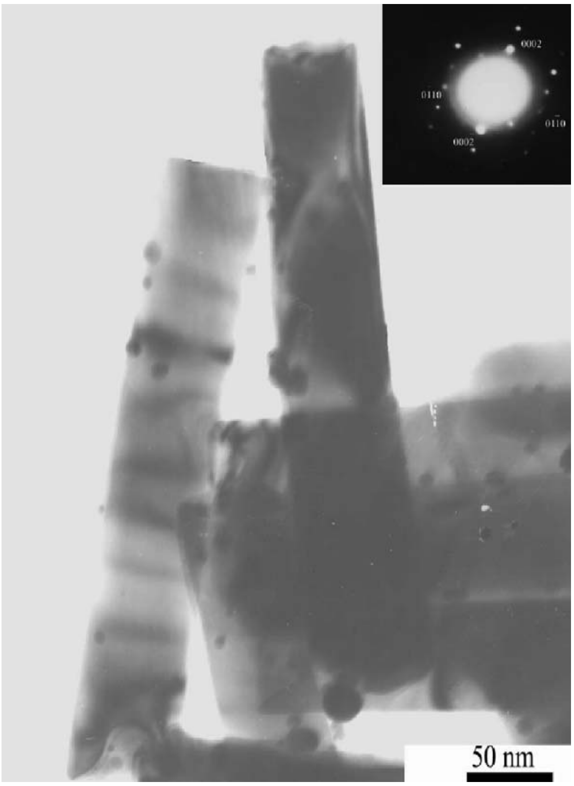

Fig. 3. TEM image of ZnS nanorods at reactor pressure of 10 Torr. The insert is the SAED pattern of a single ZnS nanorod.

equipped in our system, the plasma generation in the growth chamber is strongly dependent on growth temperature and reactor pressure. When the substrate temperature kept constant, the energy of the species in the plasma is only a function of the reactor pressure. As pressure decreases, the kinetic energy of species increases due to the enhancement in intensity of the plasma. The effect of plasmas is believed to provide an additional energy to enhance the surface mobility of the reactant radicals [25]. As reported previously [26], this increased plasma intensity lead to evolution of the surface roughness and a change of the growth mode from two- to three dimensional. Furthermore, when the plasma energy is high enough the generated plasma will damage the product, which means some unstable nucleation sites could be removed from the substrate surface. This effect will lead to the construction of special nanostructures under high-energy plasma treatment. Based on above discussion, a plasma assistant growth mechanism could be employed to explain nanorods growth. Moreover, the lattice mismatch between Al_2O_3 substrate and hexagonal ZnS is only about 3%, the small lattice mismatch allow for the preferential growth of the crystal along the *c*-axis direction. Under high growth pressure (35 Torr, low plasma energy), the migration of atoms in the surface is slight influenced on by the plasma. The initial islands will grow up to continuous larger crystalline grains, as seen in Fig. 1(a). As the growth pressure decreases, morphology of ZnS was changed from films to nanostructure because ion damage and higher migration of surface atoms. Then with further increase in the plasma energy, only some limited nucleation sites could exist, resulting in nanorods growth. Because of the effects of both high-substrate temperature and high-plasma energy, nucleation occurs almost epitaxial growth on substrate surface. As discussed above, ZnS nanorods aligned vertically well could be obtained under pressure of 10 Torr. The reactor pressure cannot be set below 10 Torr due to the limit of our MOCVD equipment.

Optical properties of ZnS nanorods was measured by the PL spectrum excited by a He–Cd laser with 325 nm line at RT, as seen in Fig. 4. A strong ultraviolet emission peak located at 335 nm was obtained from the as-grown ZnS nanorods at

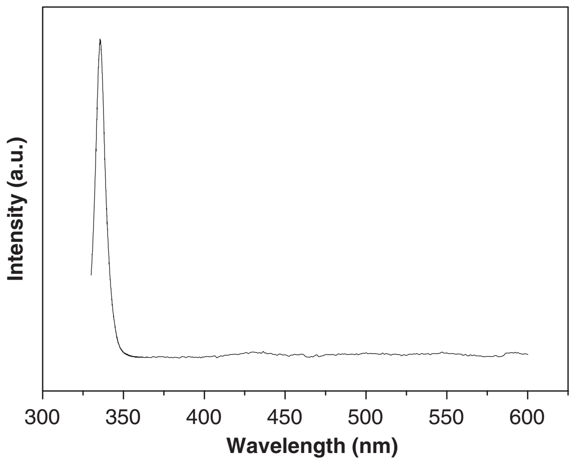

Fig. 4. The PL spectrum of the as-grown ZnS nanorods at RT.

reactor pressures of 10 Torr, which is assigned to near band-edge emission of ZnS [27]. A very weak visible emission band located at around 430 nm was also observed, which can be attributed to the existence of defect in the ZnS, such as vacancies, dislocations or surface states [24]. The strong UV peak and weak visible band provide evidence that ZnS nanorods with high structural and optical quality were obtained.

4. Conclusion

The growth of highly aligned ZnS nanorods using plasma-assisted metalorganic chemical vapor deposition at 650 °C was reported. It was found that the plasma plays an important role in the growth process and results in change of morphology of ZnS. The plasma generation was strongly dependent on growth pressure. Under the pressure of 10 Torr, well-aligned ZnS nanorods array could be obtained. FE–SEM images revealed that nanorods with uniform distributions in their diameters, lengths, and densities were grown vertically on the substrate. SAED pattern measurements show that the ZnS nanorods are single crystal with wurtzite structure in nature. The strong near band-edge PL peak and very weak visible emission reveal the good optical properties of the nanorods.

Acknowledgments

This work is supported by the "863" High Technology Research Program in China, under Grant no. 2001AA311120, the Key Project of National Natural Science Foundation of China under Grant no. 60336020, the Innovation Project of Chinese Academy of Sciences, the National Natural Science Foundation of China under Grant nos. 60278031, 60376009 and 50402016.

References

[1] C.M. Lieber, Solid State Commun. 107 (1998) 607.
[2] Xiao-Sheng Fang, Chang-Hui Ye, Xin-Sheng Peng, Yin-Hai Wang, Yu-Cheng Wu, Li-De Zhang, J. Crystal Growth 263 (2004) 263.
[3] C. Falcony, M. Garcia, A. Ortiz, J.C. Alonso, J. Appl. Phys. 72 (1992) 1525.
[4] W. Tang, D.C. Cameron, Thin Solid Films 280 (1996) 221.
[5] C.N. Xu, T. Watanabe, M. Akiyama, X.G. Zheng, Mater. Res. Bull. 34 (1999) 1491.
[6] T.V. Prevenslik, J. Lumin. 87 (2000) 1210.
[7] W. Chen, Z.G. Wang, Z.J. Lin, L.Y. Lin, Appl. Phys. Lett. 70 (1997) 1465.
[8] Ying-Chun Zhu, Yoshio Bando, Dong-Feng Xue, Appl. Phys. Lett. 82 (2003) 1769.
[9] Y. Wada, H. Yin, T. Kitamura, S. Yanagida, Chem. Commun. (Camb.) 24 (1998) 2683.
[10] Yang Jiang, Xiang-Min Meng, Ji Liu, Zhi-Yuan Xie, Chun-Sing Lee, Shuit-Tong Lee, Adv. Mater. 15 (2003) 323.
[11] Yewu Wang, Lide Zhang, Changhao Liang, Guozhong Wang, Xinsheng Peng, Chem. Phys. Lett. 357 (2002) 314.
[12] X.M. Meng, J. Liu, Y. Jiang, W.W. Chen, C.S. Lee, I. Bello, S.T. Lee, Chem. Phys. Lett. 382 (2003) 434.
[13] Daniel F. Moore, Yong Ding, Zhong Lin Wang, J. Am. Chem. Soc. 126 (2004) 14372.
[14] Shu-Hong Yu, Masahiro Yoshimura, Adv. Mater. 14 (2002) 296.
[15] Junping Li, Yao Xu, Dong Wu, Yuhan Sun, Solid State Commun. 130 (2004) 619.
[16] Ying-Chun Zhu, Yoshio Bando, Dong-Feng Xue, Appl. Phys. Lett. 82 (2003) 1769.
[17] Yong Ding, Xu Dong Wang, Zhong Lin Wang, Chem. Phys. Lett. 398 (2004) 32.
[18] Jian Xu, Yadong Li, J. Colloid Interface Sci. 259 (2003) 275.
[19] X.-M. Meng, Y. Jiang, J. Liu, C.-S. Lee, I. Bello, S.-T. Lee, Appl. Phys. Lett. 83 (2003) 2244.
[20] Xudong Wang, Puxian Gao, Jing Li, Christopher J. Summers, Zhong Lin Wang, Adv. Mater. 14 (2002) 1732.
[21] R.S. Wagner, W.C. Ellis, Appl. Phys. Lett. 4 (1964) 89.
[22] Yung-Jung Hsu, Shih-Yuan Lu, Langmuir 20 (2004) 23.
[23] Sriram Muthukumar, Haifeng Sheng, Jian Zhong, IEEE Trans. Nanotechnol. 2 (2003) 50.
[24] H.J. Yuan, S.S. Xie, D.F. Liu, X.Q. Yuan, Z.P. Zhou, L.J. Ci, J.X. Wang, Y. Gao, L. Song, L.F. Liu, W.Y. Zhou, G. Wang, J. Crystal Growth 258 (2003) 225.
[25] S.J. DeBoer, V. Dalal, G. Chumanov, R. Bartels, Appl. Phys. Lett. 66 (1995) 2528.
[26] E. Mateeva, P. Sutter, Semicond. Sci. Technol. 13 (1998) 1426.
[27] Seiji Nakamura, Takashi Sakashita, Yoichi Yamada, Tsunemasa Taguchi, J. Crystal Growth 184 (1998) 1110.